

Influence of Microbial Growth Kinetics on Steady State Multiplicity and Stability of a Two-Step Nitrification (SHARON) Model

Eveline I.P. Volcke,¹ Mihaela Sbarciog,² Mia Loccufier,² Peter A. Vanrolleghem,^{1,3} Erik J.L. Noldus²

¹BIOMATH, Department of Applied Mathematics, Biometrics and Process Control, Ghent University, Coupure links 653, B-9000 Gent, Belgium; telephone: +32 9 264 59 37; fax: +32 9 264 62 20; e-mail: eveline.volcke@biomath.ugent.be

²Department of Electrical Energy, Systems and Automation, Ghent University, Technologiepark 913, B-9052 Zwijnaarde, Belgium

³modelEAU, Département de génie civil, Pavillon Pouliot, Université Laval, G1K 7P4 Québec, QC, Canada

Received 30 October 2006; revision received 27 February 2007; accepted 6 April 2007

Published online 26 April 2007 in Wiley InterScience (www.interscience.wiley.com). DOI 10.1002/bit.21464

ABSTRACT: In this paper, the influence of microbial growth kinetics on the number and the stability of steady states for a nitrogen removal process is addressed. A two-step nitrification model is studied, in which the maximum growth rate of ammonium oxidizers is larger than the one of nitrite oxidizers. This model describes the behavior of a SHARON reactor for the treatment of wastewater streams with high ammonium concentrations. Steady states are identified through direct calculation using a canonical state space model representation, for several types of microbial kinetics. The stability of the steady states is assessed and the corresponding phase portraits are analyzed. Practical operation of a SHARON reactor aims at reaching ammonium conversion to nitrite while suppressing further conversion to nitrate. Regions in the input space are identified that result in this desired behavior, with only nitrite formation. It is demonstrated that not only the dilution rate plays a role, as is commonly known, but also the influent ammonium concentration. Besides, the type of microbial (inhibition) kinetics has a nonnegligible influence. While the results indicate that product inhibition does not affect the number of steady states of a (bio)reactor model, it is shown that substrate inhibition clearly yields additional steady states. Particular attention is devoted to the physical interpretation of these phenomena.

Biotechnol. Bioeng. 2007;98: 882–893.

© 2007 Wiley Periodicals, Inc.

KEYWORDS: modeling; nitrification; stability analysis; steady states; wastewater treatment

Introduction

In (bio)chemical reaction systems, steady state multiplicity, by which we mean that different initial reactor conditions result in different steady states reached for the same input variables, is often encountered. Experimental evidence of such behavior has been reported by several authors, for example, by Lei et al. (2003) during aerobic cultivation of *Saccharomyces cerevisiae*. As good knowledge of process dynamics is essential for design and control purposes, it has been attempted to rigorously formulate conditions under which steady state multiplicity occurs, for example, by Agrawal et al. (1982) for isothermal continuous stirred bioreactors. Whereas in a nonisothermal reacting system, the nonlinear dependence of the rate constant on temperature may contribute to system multiplicity, in isothermal systems like biological wastewater treatment systems, this multiplicity may result from nonlinear kinetics (Tong and Fan, 1988). Besides, also the phenomenon of metabolic regulation, an omnipresent feature of biochemical pathways that endows cells with the ability to make choice decisions at metabolic crossroads, leads to nonlinear behavior in bioreactors and is a source of steady state multiplicity (Namjoshi and Ramkrishna, 2001).

This paper assesses steady state multiplicity and stability of a two-step nitrification model for ammonium removal from wastewater. The model can be used to describe the

behavior of a SHARON (Single reactor High activity Ammonium Removal Over Nitrite) process (Hellings et al., 1998), that is ideally suited to remove nitrogen from wastewater streams with high ammonium concentration. The SHARON reactor is operated as a continuously stirred tank reactor (CSTR) without biomass retention. At the prevailing pH (about 7) and high temperature (30–40°C), ammonium oxidizers grow faster than nitrite oxidizers. For this reason, it is possible to establish ammonium oxidation to nitrite only and prevent further oxidation of nitrite to nitrate by setting an appropriate dilution rate. In this way, substantial savings in aeration costs are realized, in comparison with oxidation of ammonium to nitrate.

In an attempt to identify regions in the input space for which a unique steady state exists, only the wash-out state has been found—for very high values of the dilution rate (Volcke et al., 2006), which is clearly not an interesting operating point. In this contribution, the steady states of a two-step nitrification model are calculated directly in a number of simplified cases. Note that here the term “steady state” is used synonymous to “equilibrium” or “equilibrium state,” as a solution of the steady state process model. It should be stressed that these steady states are not a priori stable. Particular attention is devoted to the effect of biological conversion kinetics on the number of steady states and on their stability. Phase trajectories illustrate the process behavior. It is studied which combinations of input variables, in particular the applied dilution rate for given influent ammonium concentrations, result in ammonium oxidation to nitrite only. The influence of changing parameter and input values, reflecting the uncertainty in the description of biological systems as well in as influent characterization, is addressed briefly.

Materials and Methods

Two-Step Nitrification Model Under Study

The simplified SHARON reactor model under study considers two nitrification reactions: oxidation of ammonium to nitrite and subsequent oxidation of nitrite to nitrate, as schematically represented in Figure 1. The concentrations ($x_i(t) \geq 0$) of the following four components, involved in the biological conversion reactions, are identified as the system's state variables: (total) ammonium ($x_1 = \text{NH}_4^+ + \text{NH}_3$), (total) nitrite ($x_2 = \text{HNO}_2 + \text{NO}_2^-$), ammonium oxidizers (x_3), and nitrite oxidizers (x_4). The concentration of nitrate, which is produced during nitrite oxidation, is not taken up as a state variable of the model, as it is directly related to the amount of nitrite oxidizers (x_4) in the reactor. Although the two biological conversion reactions are essentially consecutive reactions (ammonium is first oxidized to nitrite, which is subsequently oxidized to nitrate), ammonium is consumed in both reactions: during ammonium oxidation, it serves as both the electron donor and the nitrogen source for incorporation in biomass, while

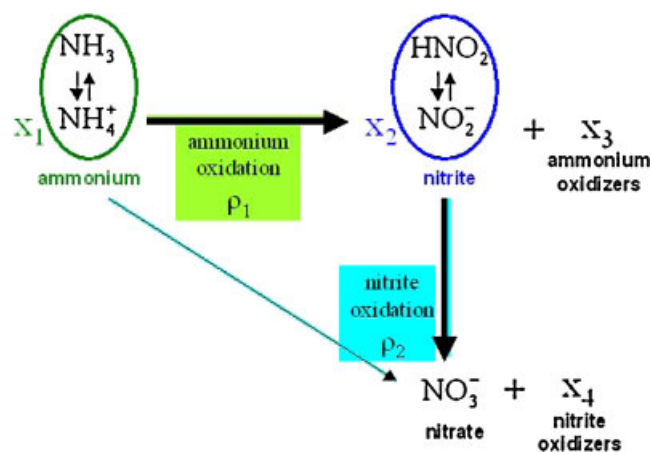


Figure 1. Basic two-step nitrification reaction scheme. [Color figure can be seen in the online version of this article, available at www.interscience.wiley.com.]

a small amount of ammonium is also consumed during nitrite oxidation, as the nitrogen source for incorporation in biomass.

The reactor is modeled as a CSTR without biomass retention. The reactor liquid volume is assumed constant. The system's state equations are given by the individual mass balances for ammonium, nitrite, ammonium oxidizers, and nitrite oxidizers (see Volcke, 2006, for details):

$$\begin{aligned} \dot{x}_1 &= u_0(u_1 - x_1) - a\rho_1(\mathbf{x}) - b\rho_2(\mathbf{x}) \equiv f_1(\mathbf{x}) \\ \dot{x}_2 &= -u_0x_2 + c\rho_1(\mathbf{x}) - d\rho_2(\mathbf{x}) \equiv f_2(\mathbf{x}) \\ \dot{x}_3 &= -u_0x_3 + \rho_1(\mathbf{x}) \equiv f_3(\mathbf{x}) \\ \dot{x}_4 &= -u_0x_4 + \rho_2(\mathbf{x}) \equiv f_4(\mathbf{x}) \end{aligned} \quad (1)$$

in which $\mathbf{x} = [x_1 \ x_2 \ x_3 \ x_4]^T$, T indicating the transposed vector. The model parameters $a = 1/Y_1$, $b = (1/Y_1) - b$, and $d = 1/Y_2$ represent constant, strictly positive stoichiometric coefficients, in which Y_1 and Y_2 denote the biomass yield coefficient on substrate during ammonium oxidation and nitrite oxidation, respectively, while b represents the nitrogen fraction in biomass. The input variables are the dilution rate ($u_0(t) \geq 0$) and the influent concentration of total ammonium ($u_1(t) \geq 0$). The influent is assumed to contain neither nitrite nor biomass. Ammonium and nitrite oxidation rates are described by their respective reaction rates, ρ_1 and ρ_2 , each proportional to the corresponding biomass concentration:

$$\begin{aligned} \rho_1 &= \mu_1x_3 \\ \rho_2 &= \mu_2x_4 \end{aligned} \quad (2)$$

Many different expressions for the microbial growth rates μ_i have been reported in literature, differing essentially in the inhibition effects acting on the nitrifying biomass. Since early reports, for example, by Anthonisen et al. (1976), it is generally accepted that ammonium (ammonia) and nitrite (nitrous acid) may inhibit both ammonium oxidation and

nitrite oxidation. These inhibition effects become particularly important when treating wastewater streams with high ammonium concentrations. However, many different values are found in literature with respect to the level of inhibition. Although some of the reported results even seem contradictory, they essentially reflect the strong capacity of nitrifying organisms to adapt to different reactor and influent conditions. For instance, while Anthonisen et al. (1976) report on inhibition of ammonium oxidation by ammonium rather than by nitrite, the model of Hellinga et al. (1999), which was based on experimental results, considers inhibition of ammonium oxidation by nitrite but not by ammonium. The latter findings have recently been experimentally confirmed by Van Hulle et al. (2007).

Regarding the different inhibition effects on nitrification reported by different literature sources, a more pragmatic approach has been decided on in this contribution. Four basic types of microbial conversion kinetics (different μ_i) have been considered to evaluate their effect on the number of steady states and their stability (Table I). This constitutes the difference between the models evaluated in this study.

The first model assumes that no inhibition of any kind takes place. Model II adds nitrite inhibition of ammonium oxidation (with inhibition constant c_1) to model I, while model III considers ammonium inhibition of ammonium oxidation (with inhibition constant d_1). Model IV accounts for nitrite inhibition of nitrite oxidation as the only form of inhibition (with constant d_2). The maximum growth rates of ammonium and nitrite oxidation (a_1 and a_2 , respectively), the substrate affinity constants (b_1 and b_2) as well as the above-mentioned inhibition constants are model parameters, which have a constant value, at least for a SHARON reactor in which temperature and pH are controlled at a fixed level, as is assumed here. Note that the terminology “maximum growth rates” has been used to denote the parameters a_1 and a_2 throughout this manuscript, although their values do not strictly correspond to the maximum values of μ_1 in case of model III and μ_2 in case of model IV, respectively. It is further assumed that oxygen is always present in excess, or at least a constant oxygen level is maintained (the influence of sub-optimal oxygen levels is then comprised in the parameters a_1 and a_2), which is a

reasonable assumption for a SHARON reactor. The numerical values for the model parameters applied in this study are summarized in Table II.

Canonical State Space Model Representation

By defining new state space variables:

$$\begin{bmatrix} y_1 \\ y_2 \\ y_3 \\ y_4 \end{bmatrix} \equiv \begin{bmatrix} x_1 + ax_3 + bx_4 \\ x_2 - cx_3 + dx_4 \\ x_3 \\ x_4 \end{bmatrix} \quad (3)$$

the two-step nitrification model defined by Equation (1) is transformed into a canonical form (Bastin and Dochain, 1990; Bastin and Van Impe, 1995), consisting of a linear part of dimension 2, dynamically coupled with a nonlinear part of dimension 2:

$$\begin{aligned} \dot{y}_1 &= u_0(u_1 - y_1) \equiv g_1(\mathbf{y}) \\ \dot{y}_2 &= -u_0 y_2 \equiv g_2(\mathbf{y}) \\ \dot{y}_3 &= (-u_0 + \lambda_1)y_3 \equiv g_3(\mathbf{y}) \\ \dot{y}_4 &= (-u_0 + \lambda_2)y_4 \equiv g_4(\mathbf{y}) \end{aligned} \quad (4)$$

with

$$\lambda_i(\mathbf{y}) = \mu_i(\mathbf{x}); \quad i = 1, 2 \quad (5)$$

in which

$$\begin{aligned} x_1 &= y_1 - ay_3 - by_4 \\ x_2 &= y_2 + cy_3 - dy_4 \\ x_3 &= y_3 \\ x_4 &= y_4 \end{aligned} \quad (6)$$

The state variables x_i ($i = 1, \dots, 4$) of the two-step nitrification model represented by Equation (1) cannot become negative. Call \mathbf{S}_y the image of $\mathcal{R}^{+,4} \equiv \{\mathbf{x} \in \mathcal{R}^4 : x_i \geq 0, \quad i = 1, \dots, 4\}$ under the transformation $\mathbf{x} \mapsto \mathbf{y}$. \mathbf{S}_y is the state space of the system defined by Equation (4). Every trajectory that starts at $t = 0$ in a point \mathbf{y}_0 of \mathbf{S}_y , stays in \mathbf{S}_y for $t \geq 0$. It subsequently converges (for

Table I. Microbial conversion kinetics for the models under study.

	Ammonium oxidation	Nitrite oxidation
Model I	$\mu_1 = a_1 \frac{x_1}{b_1 + x_1}$	$\mu_2 = \begin{cases} a_2 \frac{x_2}{b_2 + x_2} & \text{for } x_1 > 0 \\ 0 & \text{for } x_1 = 0 \end{cases}$
Model II	$\mu_1 = a_1 \frac{x_1}{b_1 + x_1} \frac{c_1}{c_1 + x_2}$	$\mu_2 = \begin{cases} a_2 \frac{x_2}{b_2 + x_2} & \text{for } x_1 > 0 \\ 0 & \text{for } x_1 = 0 \end{cases}$
Model III	$\mu_1 = a_1 \frac{x_1}{b_1 + x_1} \frac{d_1}{d_1 + x_1}, \quad \text{with } b_1 < d_1$	$\mu_2 = \begin{cases} a_2 \frac{x_2}{b_2 + x_2} & \text{for } x_1 > 0 \\ 0 & \text{for } x_1 = 0 \end{cases}$
Model IV	$\mu_1 = a_1 \frac{x_1}{b_1 + x_1}$	$\mu_2 = \begin{cases} a_2 \frac{x_2}{b_2 + x_2} \frac{d_2}{d_2 + x_2} & \text{for } x_1 > 0, \\ 0 & \text{for } x_1 = 0 \end{cases}, \quad \text{with } b_2 < d_2$

Table II. Numerical values of the SHARON model parameters (at pH = 7 at $T = 35^\circ\text{C}$).

Symbol	Value	Unit	Reference
a_1	2.1	day^{-1}	Hellinga et al. (1999)
b_1	4.73		Van Hulle et al. (2007)
	1.32*	mole m^{-3}	Carrera et al. (2004)
c_1	837	mole m^{-3}	Van Hulle et al. (2007)
a_2	1.05	day^{-1}	Hellinga et al. (1999)
b_2	0.4	mole m^{-3}	Wiesmann (1994)
d_1	3,406		Wiesmann (1994)
	36*	mole m^{-3}	Carrera et al. (2004)
d_2	106	mole m^{-3}	Wiesmann (1994)
$a = \frac{1}{Y_1}$	16	mole mole^{-1}	Y_1 from Hellinga et al. (1999)
b	0.2	mole mole^{-1}	typical textbook value
$c = \frac{1}{Y_1} - b$	15.8	mole mole^{-1}	determined by the values of a and b
$d = \frac{1}{Y_2}$	58.6	mole mole^{-1}	Y_2 from Hellinga et al. (1999)

*This value has only been applied to model III (in Figs. 5 and 6), for comparison with the default values.

positive constant input values u_0 and u_1) to the cross-section Δ of S_y with the plane $\{y_1 = u_1, y_2 = 0\}$, as can be seen from Equation 4. Δ is a bounded region, defined by the inequalities

$$\begin{aligned} u_1 - ay_3 - by_4 &\geq 0 \\ cy_3 - dy_4 &\geq 0 \\ y_3 &\geq 0 \\ y_4 &\geq 0 \end{aligned} \quad (7)$$

The process converges to a second order behavior that is determined by the dynamics of y_3 ($=x_3$) and y_4 ($=x_4$). In the sequel, a mathematical steady state solution \mathbf{y}_{ss} of Equation (4) will be called a physical steady state if it lies in S_y .

Stability Assessment Of Steady States

The linearization principle is used to investigate the local asymptotic stability of steady states. A steady state \mathbf{x}_{ss} of the two-step nitrification model (Eq. 1) is locally asymptotically stable if the eigenvalues of the Jacobian matrix:

$$\left. \frac{\partial \mathbf{f}(\mathbf{x})}{\partial \mathbf{x}} \right|_{\mathbf{x} = \mathbf{x}_{ss}} \equiv \begin{bmatrix} \left. \frac{\partial f_1}{\partial x_1} \right|_{\mathbf{x} = \mathbf{x}_{ss}} & \dots & \left. \frac{\partial f_1}{\partial x_4} \right|_{\mathbf{x} = \mathbf{x}_{ss}} \\ \vdots & & \vdots \\ \left. \frac{\partial f_4}{\partial x_1} \right|_{\mathbf{x} = \mathbf{x}_{ss}} & \dots & \left. \frac{\partial f_4}{\partial x_4} \right|_{\mathbf{x} = \mathbf{x}_{ss}} \end{bmatrix} \quad (8)$$

are all in the open left half plane, that is, have a strictly negative real part.

The stability of a steady state can also be assessed using the canonical state space model representation. A steady state \mathbf{y}_{ss} of the system represented by Equation 4 is locally asymptotically stable if all eigenvalues of the system's Jacobian matrix, evaluated for this steady state,

$\mathbf{J}(\mathbf{y}_{ss}) = \left. \frac{\partial \mathbf{g}(\mathbf{y})}{\partial \mathbf{y}} \right|_{\mathbf{y} = \mathbf{y}_{ss}}$, are in the open left half plane. It can easily be seen that $\mathbf{J}(\mathbf{y}_{ss})$ has a double eigenvalue $-\mu_0$ and that its remaining two eigenvalues are the eigenvalues of the 2-dimensional matrix

$$\mathbf{J}_{34}(\mathbf{y}_{ss}) \equiv \begin{bmatrix} \left. \frac{\partial g_3}{\partial y_3} \right|_{\mathbf{y} = \mathbf{y}_{ss}} & \left. \frac{\partial g_3}{\partial y_4} \right|_{\mathbf{y} = \mathbf{y}_{ss}} \\ \left. \frac{\partial g_4}{\partial y_3} \right|_{\mathbf{y} = \mathbf{y}_{ss}} & \left. \frac{\partial g_4}{\partial y_4} \right|_{\mathbf{y} = \mathbf{y}_{ss}} \end{bmatrix} \quad (9)$$

The linearization principle provides a necessary and sufficient condition for local asymptotic stability for so-called *hyperbolic* steady states, of which the Jacobian matrix has no eigenvalues on the imaginary axis.

In case the system possesses only one asymptotically stable steady state \mathbf{y}_{ss} (besides potential unstable steady states), which is lying on the boundary of the canonical state space S_y , this steady state is also globally asymptotically stable within the physical boundaries of the system. This results from the fact that every trajectory inside a bounded region, for a second order system, should converge to either a steady state, or a limit cycle, taking into account that a limit cycle cannot surround a region containing no steady states and no limit cycle can occur around a steady state that is lying on the boundary of S_y , since this would imply that a trajectory is leaving the system's state space. In case the system possesses only one asymptotically stable steady state \mathbf{y}_{ss} , not lying on the boundary of the canonical state space, the absence of limit cycles should be verified through simulation.

Results and Discussion

This contribution aims at identifying the number of steady states, corresponding with constant input values u_0 (the dilution rate) and u_1 (the influent ammonium concentration), as well as assessing the stability of these steady states for the simplified reactor models under study. It is however worthwhile to mention that some general conclusions can be drawn for extreme values of the dilution rate u_0 and/or the influent ammonium concentration u_1 , without explicitly knowing the expression of the microbial kinetics.

Steady State Behavior In Case $u_0 = 0$ Or $u_0 = +\infty$

In case $u_0 = 0$, that is, the reactor is operated as a batch reactor, Equation (1) yields an infinite number of steady state solutions \mathbf{x}_{ss} for the conversion kinetics of Equation (2) and Table I:

- $x_{ss1} = 0$; $x_{ss2}, x_{ss3}, x_{ss4}$ arbitrary: there is no ammonium (left) in the reactor;
- $x_{ss2} = x_{ss3} = 0$; x_{ss1}, x_{ss4} arbitrary: neither nitrite nor ammonium oxidizers are present in the reactor;
- $x_{ss3} = x_{ss4} = 0$; x_{ss1}, x_{ss2} arbitrary: no biomass is present in the reactor.

The initial reactor conditions determine which steady state will be reached.

On the other hand, for an infinitely large dilution rate ($u_0 \rightarrow +\infty$), Equation (1) give rise to a unique steady state, corresponding with the influent conditions: $\mathbf{x}_{ss} = [u_1 \ 0 \ 0 \ 0]^T$, that is, the wash-out point where the reactor fails. Using the linearization principle, it follows straightforwardly that this wash-out point for $u_0 \rightarrow +\infty$ is always locally asymptotically stable (Volcke, 2006). For realistic values of u_0 in between these limits, no general conclusions can be drawn regarding the number of steady states without explicitly defining the structure of the microbial kinetics.

Steady State Behavior In Case $u_1 = 0$

In case the reactor influent does not contain ammonium ($u_1 = 0$), it follows from Equations (6) and (8) that

$$\begin{aligned} \dot{\mathbf{y}} = \mathbf{0} &\Leftrightarrow y_{ss1} = y_{ss2} = y_{ss3} = y_{ss4} = 0 \Leftrightarrow \\ x_{ss1} &= x_{ss2} = x_{ss3} = x_{ss4} = 0 \end{aligned}$$

indicating a unique (trivial) steady state corresponding with biomass washout.

Steady State Behavior in Case $u_0 > 0$ and $u_1 > 0$

As no general conclusions can be drawn on the number of steady states for dilution rates $0 < u_0 < +\infty$, their values will be calculated directly in four cases of simplified microbial kinetics (Table I). This calculation is substantially simplified using the canonical state space model representation (Eq. 4).

In case $u_0 > 0$ and $u_1 > 0$, no steady state exists for which the ammonium concentration is zero ($x_{ss1} = 0$). Indeed, $x_{ss1} = 0$ implies that $\lambda_1(\mathbf{y}_{ss}) = \lambda_2(\mathbf{y}_{ss}) = 0$ (Table I and Eq. 6), so $y_{ss3} = y_{ss4} = 0$ (Eq. 4 for $u_0 \neq 0$) and consequently $y_{ss1} = 0$ (Eq. 3), which requires $u_0 u_1 = 0$ (Eq. 4). As a result, in equilibrium the nontrivial expressions for μ_2 ($\mu_2 \neq 0$) in Table I hold, so the steady states fulfill the following set of equations (see Eq. 4):

$$\begin{aligned} y_{ss1} &= u_1 \\ y_{ss2} &= 0 \\ (-u_0 + \lambda_1(\mathbf{y}_{ss}))y_{ss3} &= 0 \\ (-u_0 + \lambda_2(\mathbf{y}_{ss}))y_{ss4} &= 0 \end{aligned} \quad (10)$$

From the definition of x_2 (Eq. 6) where $y_{ss2} = 0$ and the physical boundary conditions $x_2 \geq 0$ and $y_4 \geq 0$, it results that $y_{ss3} = 0$ (no ammonium oxidizers) also implies $y_{ss4} = 0$ (no nitrite oxidizers). This seems logical regarding the fact that, in a SHARON reactor, ammonium oxidizers grow faster than nitrite oxidizers. Consequently, three different types of steady states are obtained:

1. $y_{ss3} = y_{ss4} = 0$ This steady state corresponds with complete biomass wash-out.

2. $y_{ss4} = 0$ while $y_{ss3} \neq 0$ In this case, no nitrite oxidizers are present and consequently no nitrate is formed, as is typically aimed for in a SHARON reactor. The dilution rate equals the growth rate of ammonium oxidizers, $u_0 = \lambda_1$, and one or more steady states with only nitrite formation result from this expression, depending on the microbial kinetics (see further).

3. $y_{ss3} \neq 0$ and $y_{ss4} \neq 0$ In this case, both ammonium oxidizers and nitrite oxidizers are present, so at least part of the formed nitrite is further oxidized to nitrate. Now the growth rates of ammonium oxidizers and nitrite oxidizers are equal and also equal the dilution rate: $u_0 = \lambda_1 = \lambda_2$. Again, the number of corresponding steady states depends on the microbial kinetics (see further).

In what follows, the number of steady states, the conditions under which they occur (i.e., are physical steady states in the sense that they fulfill Eq. 7) as well as their stability is assessed for the different models under study. All steady state values are expressed in the \mathbf{x} -space, calculated straightforwardly from the obtained values in the \mathbf{y} -space through Equation (3). Detailed calculations can be found in Volcke (2006).

Model I: No Inhibition

In this case, up to three steady states occur, although in all cases only one steady state is (quasi) globally asymptotically stable (Table III). While the wash-out state $\mathbf{x}_{ss}^{A,I}$ always occurs, the remaining two steady states only represent physical states under certain conditions. For a SHARON reactor, in which the maximum growth rate of ammonium oxidizers is larger than the maximum growth rate of nitrite oxidizers ($a_1 > a_2$), condition 12 for the occurrence of a steady state in which nitrate is formed ($\mathbf{x}_{ss}^{C,I}$) is clearly more stringent than condition 11 for the occurrence of a steady state with only nitrite formation ($\mathbf{x}_{ss}^{B,I}$). Note that $x_{ss1}^{B,I} = x_{ss1}^{C,I}$, which means that the ammonium concentration is the same for both steady states.

Figure 2 depicts the occurrence of steady states in terms of the dilution rate u_0 and the influent ammonium concentration u_1 . The corresponding phase trajectories (in Δ) are depicted in Figure 3. For high dilution rates u_0 or low influent ammonium concentrations u_1 , that is, when Equation (11) is not fulfilled (zone A), only the wash-out state $\mathbf{x}_{ss}^{A,I}$ is a physical steady state and is globally asymptotically stable within the physical boundaries. For moderately high dilution rates u_0 and somewhat high influent ammonium concentrations u_1 , that is, Equation (11) is fulfilled but not Equation 12 (zone AB), the system possesses two physical steady states. The wash-out state $\mathbf{x}_{ss}^{A,I}$ is now unstable. The steady state $\mathbf{x}_{ss}^{B,I}$ (only nitrite formation) is *quasi* globally asymptotically stable, in the sense that all trajectories within the physical boundaries of the system converge to this point, except the trivial trajectory coinciding with $\mathbf{x}_{ss}^{A,I}$ (initially no biomass present

Table III. Values, occurrence and stability of steady states for a model without inhibition (model I).

Symbol	Type	Value	Occurrence	Stability
$x_{ss}^{A,I}$	Wash-out	$\begin{bmatrix} u_1 \\ 0 \\ 0 \\ 0 \end{bmatrix}$	Always	Zone A: g.a.s. Zones AB and ABC: unstable
$x_{ss}^{B,I}$	Only nitrite formation	$\begin{bmatrix} \frac{b_1 u_0}{a_1 - u_0} \\ \frac{c}{a} \left(u_1 - \frac{b_1 u_0}{a_1 - u_0} \right) \\ \frac{1}{a} \left(u_1 - \frac{b_1 u_0}{a_1 - u_0} \right) \\ 0 \end{bmatrix}$	if $u_0 < \frac{a_1 u_1}{b_1 + u_1}$ \Leftrightarrow if $u_1 > \frac{b_1 u_0}{a_1 - u_0}$ and $u_0 < a_1$	(11) Zone AB: quasi g.a.s. Zone ABC: unstable
$x_{ss}^{C,I}$	Nitrate formation	$\begin{bmatrix} \frac{b_1 u_0}{a_1 - u_0} \\ \frac{b_2 u_0}{a_2 - u_0} \\ \frac{d(u_1 - x_{ss1}^{C,I}) + b x_{ss2}^{C,I}}{ad + bc} \\ \frac{c(u_1 - x_{ss1}^{C,I}) - a x_{ss2}^{C,I}}{ad + bc} \end{bmatrix}$	if $u_0 < \frac{a_2(c/a)(u_1 - ((b_1 u_0)/(a_1 - u_0)))}{b_2 + c/a(u_1 - ((b_1 u_0)/(a_1 - u_0)))}$ \Leftrightarrow if $u_1 > \frac{b_1 u_0}{a_1 - u_0} + \frac{a}{c} \frac{b_2 u_0}{a_2 - u_0}$ and $u_0 < a_2$	(12) Zone ABC: quasi g.a.s.

in the reactor, which is clearly a purely theoretical case). For sufficiently low dilution rates u_0 and corresponding influent ammonium concentrations u_1 , for which Equation 12 is fulfilled (zone ABC), three steady states occur. The wash-out state $x_{ss}^{A,I}$ is still unstable, as is now also the second steady state, $x_{ss}^{B,I}$, corresponding with only nitrite formation: only trajectories on the x_3 -axis converge to $x_{ss}^{B,I}$, corresponding with a reactor in which initially only ammonium oxidizers are present (the latter again being a purely theoretical condition). Under the same conditions, the third steady state, $x_{ss}^{C,I}$, corresponding with nitrate formation, is quasi

globally asymptotically stable, in the sense that all trajectories within the physical boundaries of the system converge to this point, except for the steady state $x_{ss}^{A,I}$ and the trajectories on the x_3 -axis.

Model II: Nitrite Inhibition of Ammonium Oxidation

Adding nitrite inhibition of ammonium oxidation to the model does not affect the number of steady states, neither their stability, although the position of the steady states corresponding with biomass growth changes, in the sense that less ammonium is converted (see Table IV). Regarding the steady state with only nitrite production, in case ammonium oxidation is inhibited by nitrite, the corresponding ammonium concentration will be higher ($x_{ss1}^{B,II} > x_{ss1}^{B,I}$) and the nitrite concentration will be lower ($x_{ss2}^{B,II} < x_{ss2}^{B,I}$) than in case no inhibition takes place. As for the steady state with nitrate production, it is clear that less ammonium will be converted ($x_{ss1}^{C,II} > x_{ss1}^{C,I}$, taking into account $\phi(u_0) > u_0$) but the same amount of nitrite will be formed ($x_{ss2}^{C,II} = x_{ss2}^{C,I}$), so less nitrate will be produced compared to the case without inhibition.

It can also be noted that the ammonium concentration corresponding with the steady state with nitrate formation is lower than in case only nitrite is formed ($x_{ss1}^{C,II} < x_{ss1}^{B,II}$): if some nitrite is further oxidized to nitrate, more ammonium can be converted in case of nitrite inhibition of ammonium oxidation.

While nitrite inhibition of ammonium oxidation does not affect the condition for the occurrence of a steady state with only nitrite production (Eq. 11), the condition for the third steady state to be a physical state becomes more stringent

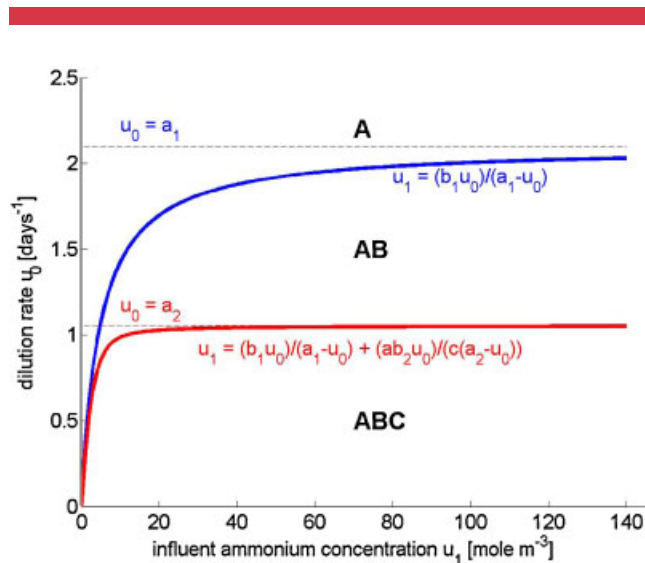


Figure 2. Steady states for a model without inhibition (model I). [Color figure can be seen in the online version of this article, available at www.interscience.wiley.com.]

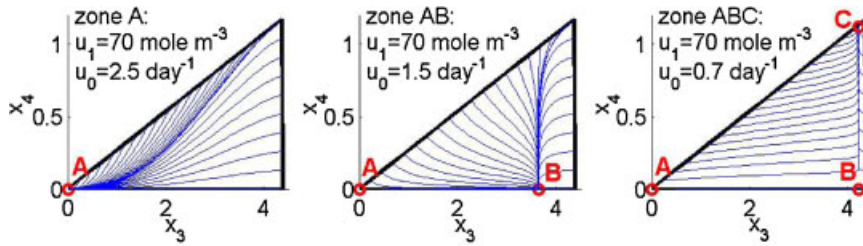


Figure 3. Trajectory fields for a model without inhibition (model I). [Color figure can be seen in the online version of this article, available at www.interscience.wiley.com.]

(condition 13 compared to condition 12, as $\phi(u_0) > u_0$). As a result, the region AB increases: only nitrite formation is obtained in a wider range, even for lower dilution rates and higher influent ammonium concentrations than in case no inhibition takes place (although this effect is almost not visible in Fig. 4 compared to Fig. 2). This effect increases for stronger inhibition values. In case there is no nitrite inhibition ($c_1 = +\infty$), conditions 12 and 13 are identical, so a continuous transient exists between model I and model II.

Model III: Ammonium Inhibition of Ammonium Oxidation

While product (nitrite) inhibition of ammonium oxidation leaves the number of steady states unchanged in comparison with a model without inhibition, substrate (ammonium)

inhibition of the ammonium oxidation—combined with substrate limitation, resulting in Haldane kinetics—does affect the number of steady states. Up to five steady states are obtained: one wash-out point ($x_{ss}^{A,III}$), two steady states corresponding with only nitrite formation ($x_{ss}^{B,III}$ and $x_{ss}^{C,III}$) and two steady states corresponding with nitrate formation ($x_{ss}^{D,III}$ and $x_{ss}^{E,III}$) (see Table V).

Figure 5 depicts the occurrence of steady states in terms of the dilution rate u_0 and the influent ammonium concentration u_1 for two different levels of ammonium inhibition. The value of $d_1 = 3,406 \text{ mole m}^{-3}$ (Wiesmann, 1994) corresponds with weak ammonium inhibition. In this case, maximally three steady states simultaneously occur in the range of influent ammonium concentrations u_1 that can reasonably be expected (typically up to 1.5 kgN m^{-3}

Table IV. Values, occurrence and stability of steady states for a model with nitrite inhibition of ammonium oxidation (model II).

Symbol	Type	Value	Occurrence	stability
$x_{ss}^{A,II}$	Wash-out	$\begin{bmatrix} u_1 \\ 0 \\ 0 \\ 0 \end{bmatrix}$	Always	Zone A: g.a.s. Zones AB and ABC: unstable
$x_{ss}^{B,II}$	Only nitrite formation	$\begin{bmatrix} x_{ss1}^{B,II} \\ \frac{c}{a}(u_1 - x_{ss1}^{B,II}) \\ \frac{1}{a}(u_1 - x_{ss1}^{B,II}) \\ 0 \end{bmatrix}$ ^(a)	if $u_0 < \frac{a_1 u_1}{b_1 + u_1}$ \Leftrightarrow if $u_1 > \frac{b_1 u_0}{a_1 - u_0}$ and $u_0 < a_1$	Zone AB: quasi g.a.s. Zone ABC: unstable
$x_{ss}^{C,II}$	Nitrate formation	$\begin{bmatrix} \frac{b_1 \phi(u_0)}{a_1 - \phi(u_0)} \\ \frac{b_2 u_0}{a_2 - u_0} \\ \frac{d(u_1 - x_{ss1}^{C,II}) + b x_{ss2}^{C,II}}{ad + bc} \\ \frac{c(u_1 - x_{ss1}^{C,II}) - a x_{ss2}^{C,II}}{ad + bc} \end{bmatrix}$ ^(b)	if $u_1 > \frac{b_1 \phi(u_0)}{a_1 - \phi(u_0)} + \frac{a}{c} \frac{b_2 u_0}{a_2 - u_0}$ and $u_0 < \hat{u}_0$ ^(c) (13)	Zone ABC: quasi g.a.s.

^aIn which $x_{ss1}^{B,II}$ is obtained from $a_1 \frac{x_{ss1}^{B,II}}{b_1 + x_{ss1}^{B,II}} \frac{c_1}{c_1 + \frac{c}{a}(u_1 - x_{ss1}^{B,II})} = u_0$.

^bWith $\phi(u_0) = u_0 + \frac{b_2 u_0^2}{c_1(a_2 - u_0)}$.

^cWith \hat{u}_0 from $\phi(\hat{u}_0) = a_1$; $0 < \hat{u}_0 < a_2$.

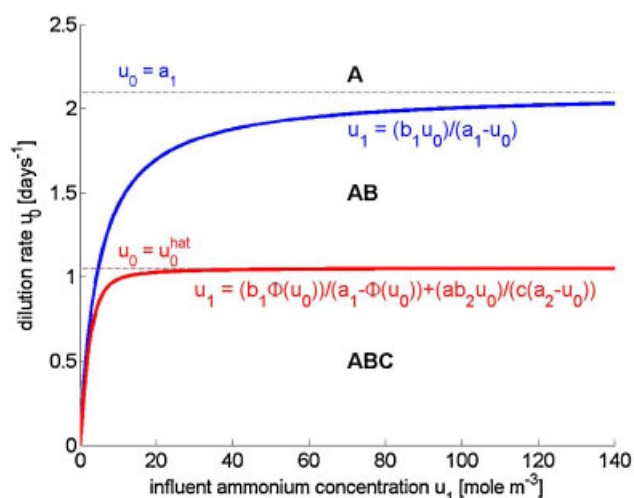


Figure 4. Steady states for a model with nitrite inhibition of ammonium oxidation (model II). [Color figure can be seen in the online version of this article, available at www.interscience.wiley.com.]

$\approx 100 \text{ mole m}^{-3}$ for reject water, although other types of wastewater streams such as thin manure fractions or landfill leachate may contain up to twice this value). In the region $u_1 = [0, 100]$, the behavior is qualitatively the same as for the models I (Fig. 2) and II (Fig. 4). However, if stronger ammonium inhibition of ammonium oxidation would prevail, up to five steady states could occur at the same time. This has been depicted in Figure 5 for $b_1 = 1.32 \text{ mole m}^{-3}$; $d_1 = 36 \text{ mole m}^{-3}$, corresponding to the values reported by Carrera et al. (2004) for suspended cells, after conversion to $\text{pH} = 7$ at $T = 35^\circ\text{C}$, as assumed in this study.

Figure 6 gives the phase trajectories for the distinguished operating regions (for $b_1 = 1.32 \text{ mole m}^{-3}$; $d_1 = 36$

mole m^{-3}). In the operating zones A, AB, and ABD, the stability of the steady states is the same as for the corresponding zones in the models I and II without nitrite inhibition—only one stable steady state occurs at a time (note however that zone ABD for model III corresponds with zone ABC for models I and II). In contrast, the operating zones ABC, ABCD, and ABCDE, in which a second steady state corresponding with only nitrite production ($\mathbf{x}_{\text{ss}}^{\text{C,III}}$) occurs, possess two steady states that are locally asymptotically stable: the wash-out state and a nontrivial one. The stability boundary, that separates their attraction regions, determines from which initial states the process will converge to which steady state. In the operating zones ABC and ABCD, only trajectories parallel to the x_4 -axis and with $x_{\text{ss}3}^{\text{C,III}}$ as the x_3 -coordinate, converge to the unstable state $\mathbf{x}_{\text{ss}}^{\text{C,III}}$ (Volcke, 2006), meaning that this steady state (with only nitrite formation) will only be reached if the initial amount of ammonium oxidizers in the system is exactly the same as for $\mathbf{x}_{\text{ss}}^{\text{C,III}}$. These trajectories separate the regions of attraction of the two steady states that are both locally asymptotically stable: $\mathbf{x}_{\text{ss}}^{\text{A,III}}$ (wash-out) and $\mathbf{x}_{\text{ss}}^{\text{B,III}}$ (only nitrite production) in zone ABC; $\mathbf{x}_{\text{ss}}^{\text{A,III}}$ and $\mathbf{x}_{\text{ss}}^{\text{D,III}}$ (nitrate production) in zone ABCD. The remaining steady state $\mathbf{x}_{\text{ss}}^{\text{B,III}}$ in zone ABCD, also corresponding with only nitrite formation, is unstable and will only be reached if initially only ammonium oxidizers are present in the system, *in a sufficient amount*: only trajectories on the x_3 -axis to the right of $\mathbf{x}_{\text{ss}}^{\text{B,III}}$ converge to $\mathbf{x}_{\text{ss}}^{\text{B,III}}$. In case the system possesses five steady states (operating zone ABCDE), only $\mathbf{x}_{\text{ss}}^{\text{A,III}}$ (wash-out) and $\mathbf{x}_{\text{ss}}^{\text{D,III}}$ (nitrate formation) are locally asymptotically stable. Their regions of attraction are separated by the trajectories that converge to the unstable steady state $\mathbf{x}_{\text{ss}}^{\text{E,III}}$ (nitrate formation). The exact location of this stability boundary is not obvious as for zones ABC and ABCD but should be estimated, for example, by a trajectory

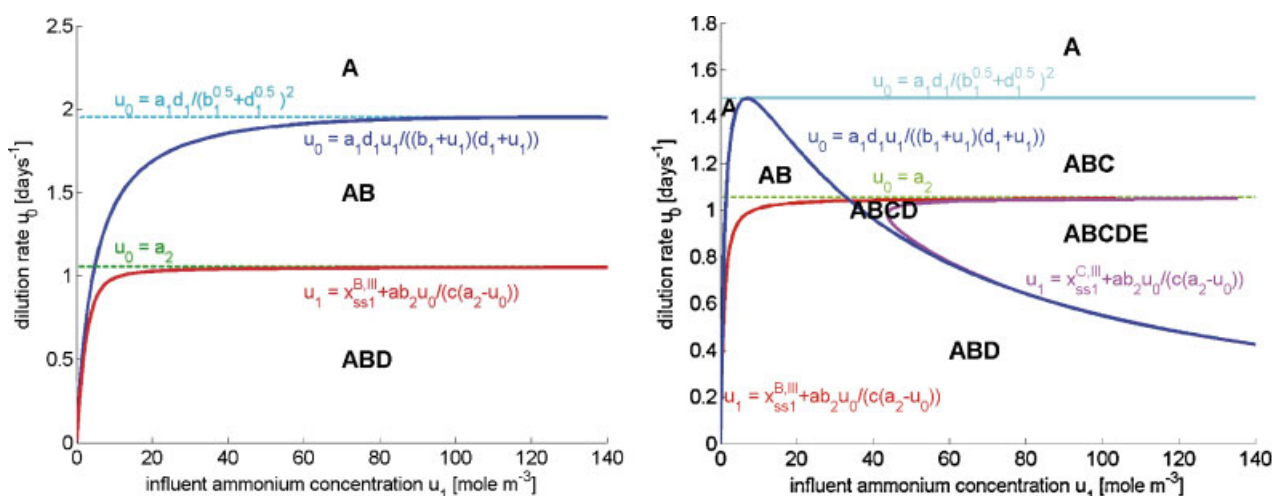


Figure 5. Steady states for a model with ammonium inhibition of ammonium oxidation (model III), for relative weak (left, $b_1 = 4.73 \text{ mole m}^{-3}$; $d_1 = 3406 \text{ mole m}^{-3}$) and strong inhibition (right, $b_1 = 1.32 \text{ mole m}^{-3}$; $d_1 = 36 \text{ mole m}^{-3}$). [Color figure can be seen in the online version of this article, available at www.interscience.wiley.com.]

Table V. Values, occurrence and stability of steady states for a model with ammonium inhibition of ammonium oxidation (model III).

Symbol	Type	Value	Occurrence	Stability
$x_{ss}^{A,III}$	Wash-out	$\begin{bmatrix} u_1 \\ 0 \\ 0 \\ 0 \end{bmatrix}$	Always	Zone A: g.a.s. Zones AB and ABD: unstable Zones ABC, ABCD, and ABCDE: l.a.s.
$x_{ss}^{B,III}$ and $x_{ss}^{C,III}$	Only nitrite formation	$\begin{bmatrix} x_{ss1}^{\alpha,III} \\ \frac{c}{a}(u_1 - x_{ss1}^{\alpha,III}) \\ \frac{1}{a}(u_1 - x_{ss1}^{\alpha,III}) \\ 0 \end{bmatrix}^{(d)}$	if $u_0 < \frac{a_1 d_1}{(\sqrt{b_1} + \sqrt{d_1})^2}$ (14) and $x_{ss1}^{\alpha,III} < u_1$ (15)	$x_{ss}^{B,III}$ Zone AB: quasi g.a.s. Zone ABC: l.a.s. Zones ABD, ABCD, and ABCDE: unstable
$x_{ss}^{D,III}$ and $x_{ss}^{E,III}$	Nitrate formation	$\begin{bmatrix} x_{ss1}^{\beta,III} \\ \frac{b_2 u_0}{a_2 - u_0} \\ \frac{d(u_1 - x_{ss1}^{\beta,III}) + b x_{ss2}^{\beta,III}}{ad + bc} \\ \frac{c(u_1 - x_{ss1}^{\beta,III}) - a x_{ss2}^{\beta,III}}{ad + bc} \end{bmatrix}^{(e)}$	if $u_0 < \frac{a_1 d_1}{(\sqrt{b_1} + \sqrt{d_1})^2}$ (14) and $u_0 < a_2$ (16) and $x_{ss1}^{\beta,III} < u_1 - \frac{a}{c} \frac{b_2 u_0}{a_2 - u_0}$ (17)	$x_{ss}^{D,III}$ Zone ABD: quasi g.a.s. ABCD and ABCDE: l.a.s.

^d α denotes B or C, $x_{ss1}^{\alpha,III}$ is obtained from $a_1 \frac{x_{ss1}^{\alpha,III}}{b_1 + x_{ss1}^{\alpha,III}} \frac{d_1}{d_1 + x_{ss1}^{\alpha,III}} = u_0$, say $x_{ss1}^{B,III} < x_{ss1}^{C,III}$.

^e β denotes D or E, $x_{ss1}^{\beta,III} = x_{ss1}^{\alpha,III}$, say $x_{ss1}^{D,III} < x_{ss1}^{E,III}$, so $x_{ss1}^{D,III} = x_{ss1}^{B,III}$ and $x_{ss1}^{E,III} = x_{ss1}^{C,III}$.

reversing technique (Genesis et al., 1985; Loccufier and Noldus, 2000).

Comparing these results with the ones for model I and II, it can be concluded that the main impact of ammonium inhibition of ammonium oxidation lies in the fact that, for not too low influent ammonium concentrations, the wash-out steady state is asymptotically stable and will be reached if the initial amount of ammonium oxidizers is not sufficient, even for relatively low dilution rates (zones ABC, ABCD, and ABCDE). The region in the input space for which only nitrite is formed, is smaller in case of ammonium inhibition of ammonium oxidation than in case of no inhibition

(region AB, Fig. 2 vs. Fig. 5), due to a downward shift of the A/AB-boundary, and is gradually reduced as this inhibition level increases, that is, as d_1 decreases. This remains true when considering that only nitrite formation will also be realized in the input region ABC for model III starting from appropriate initial reactor conditions, that is, provided that sufficient ammonium oxidizers are present. The zone in the input space for which nitrate is formed in case of no inhibition (model I, zone ABC, Fig. 2) more or less corresponds to the zone for which stable nitrate formation is possible in case ammonium oxidation is inhibited by ammonium (model III, zones ABD, ABCD, and ABCDE,

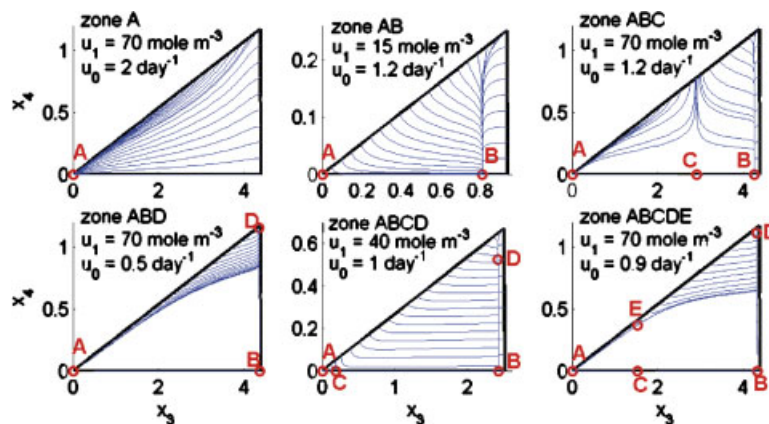


Figure 6. Trajectory fields for a model with ammonium inhibition of ammonium oxidation (model III, $b_1 = 1.32 \text{ mole m}^{-3}$; $d_1 = 36 \text{ mole m}^{-3}$). [Color figure can be seen in the online version of this article, available at www.interscience.wiley.com.]

Table VI. Values, occurrence and stability of steady states for a model with nitrite inhibition of nitrite oxidation (model IV).

Symbol	Type	Value	Occurrence	Stability
$x_{ss}^{A,IV}$	Wash-out	$\begin{bmatrix} u_1 \\ 0 \\ 0 \\ 0 \end{bmatrix}$	Always	Zone A: g.a.s. Zones AB, ABC, and ABCD: unstable
$x_{ss}^{B,IV}$	Only nitrite formation	$\begin{bmatrix} \frac{b_1 u_0}{a_1 - u_0} \\ \frac{c}{a} \left(u_1 - \frac{b_1 u_0}{a_1 - u_0} \right) \\ \frac{1}{a} \left(u_1 - \frac{b_1 u_0}{a_1 - u_0} \right) \\ 0 \end{bmatrix}$	if $u_0 < \frac{a_1 u_1}{b_1 + u_1}$ \Leftrightarrow (11) if $u_1 > \frac{b_1 u_0}{a_1 - u_0}$ and $u_0 < a_1$	Zone AB: quasi g.a.s. Zone ABC: unstable Zone ABCD: l.a.s.
$x_{ss}^{C,IV}$ and $x_{ss}^{D,IV}$	Nitrate formation	$\begin{bmatrix} \frac{b_1 u_0}{a_1 - u_0} \\ x_{ss2}^{\gamma,IV} \\ \frac{d(u_1 - x_{ss1}^{\gamma,IV}) + b x_{ss2}^{\gamma,IV}}{ad+bc} \\ \frac{c(u_1 - x_{ss1}^{\gamma,IV}) - a x_{ss2}^{\gamma,IV}}{ad+bc} \end{bmatrix}$	if $u_0 < \frac{a_1 u_1}{b_1 + u_1}$ (11) and if $u_0 < \frac{a_2 d_2}{(\sqrt{b_2} + \sqrt{d_2})^2}$ (18) and if $x_{ss2}^{\gamma,IV} < \frac{c}{a}(u_1 - x_{ss1}^{\gamma,IV})$ (19)	$x_{ss}^{C,IV}$ Zone ABC: quasi g.a.s. Zone ABCD: l.a.s. $x_{ss}^{D,IV}$ Zone ABCD: unstable

γ denotes C or D, $x_{ss2}^{\gamma,IV}$ is obtained from $a_2 \frac{x_{ss2}^{\gamma,IV}}{b_2 + x_{ss2}^{\gamma,IV}} \frac{d_2}{d_2 + x_{ss2}^{\gamma,IV}} = u_0$, say $x_{ss2}^{C,IV} < x_{ss2}^{D,IV}$.

Fig. 5). However, in the latter case wash-out may also occur if insufficient ammonium oxidizers are initially present in the reactor (for zones ABCD and ABCDE, Fig. 5).

Model IV: Nitrite Inhibition of Nitrite Oxidation

In order to further test to which extent substrate inhibition influences the number of steady states, a model with substrate inhibition of nitrite oxidation, that is, nitrite inhibition (model IV), has also been studied. It has been found that up to four physical steady states can occur (see Table VI): the wash-out state ($x_{ss}^{A,IV}$), a steady state corresponding with only nitrite formation and two steady states in which nitrate is formed. The value of the steady state corresponding with nitrite formation is exactly the same as for model I, which does not consider inhibition effects. The steady states with nitrate formation correspond with the same ammonium conversion as the one with only nitrite formation for the same model, which is also the same as for the model without inhibition (model I). It can however be shown that, in case of nitrite inhibition of nitrite oxidation (model IV), the steady state with nitrate formation corresponds with higher nitrite concentrations (so less nitrate formed) than in case of no inhibition (model I): $x_{ss2}^{\gamma,IV} > x_{ss2}^{C,I}$ for both $\gamma = C$ and D .

Figure 7 shows the different operating regions for the given parameter set. The corresponding phase trajectories are displayed in Fig. 8. In case of low dilution rates and accordingly high influent ammonium concentrations, up to four steady states can occur at the same time (operating zone ABCD, Fig. 7), of which two are locally asymptotically stable

(Table VI): $x_{ss}^{B,IV}$, corresponding with only nitrite formation and $x_{ss}^{C,IV}$, in which nitrate is formed. It is interesting to note the difference with model III, where in case of two locally asymptotic steady states, the wash-out state is always one of them. In zone ABCD, the steady state $x_{ss}^{B,IV}$ is reached and thus nitrate formation is suppressed if the initial amount of nitrite oxidizers (x_4) in the system is sufficiently low. This can be understood as a small amount of nitrite oxidizers will not be able to convert the nitrite that is built up in the system

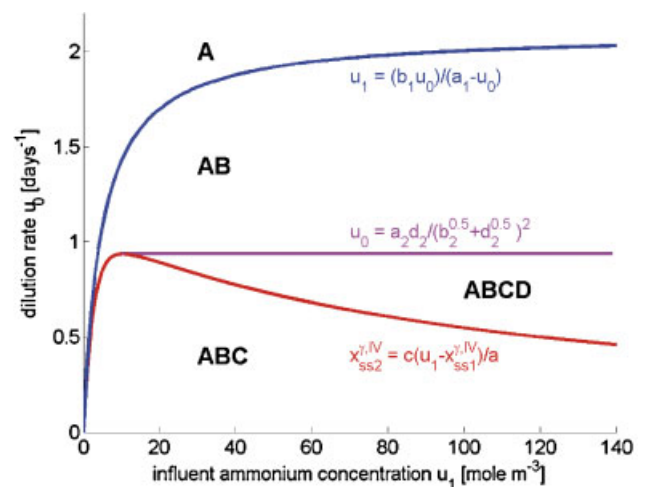


Figure 7. Steady states for a model with nitrite inhibition of nitrite oxidation (model IV). [Color figure can be seen in the online version of this article, available at www.interscience.wiley.com.]

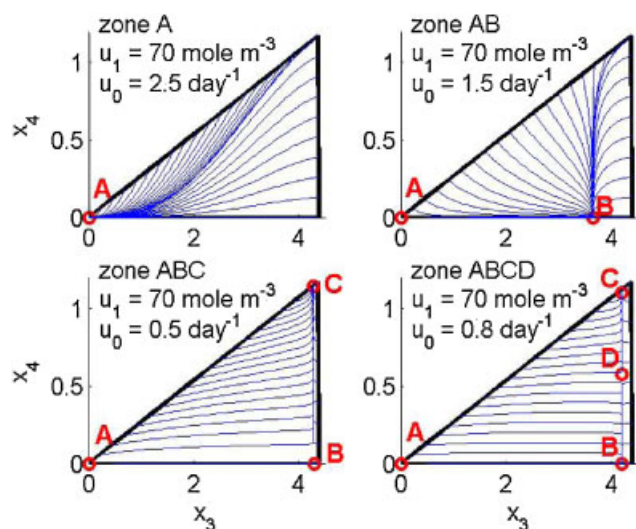


Figure 8. Trajectory fields for a model with nitrite inhibition of nitrite oxidation (model IV). [Color figure can be seen in the online version of this article, available at www.interscience.wiley.com.]

fast enough to prevent its own inhibition by nitrite, resulting in their wash-out from the reactor. In case of a high initial amount of nitrite oxidizers, the steady state $\mathbf{x}_{ss}^{C,IV}$ with nitrate formation is reached. The regions of attraction of the stable steady states $\mathbf{x}_{ss}^{B,IV}$ and $\mathbf{x}_{ss}^{C,IV}$ are separated by the trajectories which converge to the unstable steady state $\mathbf{x}_{ss}^{D,IV}$. Its exact location can only be estimated, for example, by a trajectory reversing technique, as applied by Sbarciog et al. (2006).

Overall, the operating region in which only nitrite is formed, as is the aim of a SHARON reactor, is larger in case of nitrite inhibition of nitrite oxidizers (model IV) than in case of no inhibition (model I): the steady state with only nitrite formation ($\mathbf{x}_{ss}^{B,IV}$) is reached in operating zone AB as well as in operating zone ABCD, provided the initial amount of nitrite oxidizers is sufficiently low.

Influence of Uncertainty in Parameter and Input Values

For biological systems, it is often difficult to accurately determine the parameter values. Also, parameter values may change in time, for example, because of biomass adaptation. Besides, the input values may be uncertain. The question arises to which extent this uncertainty influences the presented results.

From the analysis in the previous sections, it is clear that the model structure, in particular the type of inhibition that takes place, affects the number of steady states. It should however be noted that the exact value of the corresponding inhibition constants will not qualitatively influence this behavior. Even between different model structures, smooth transitions exist: the behavior of a reactor with relatively small biomass inhibition effects is comparable to the one of a

reactor without inhibition. As a result, it is sufficient to know parameter values within a certain range of accuracy.

Regarding the uncertainty in input values, the influence of changing dilution rates u_0 and influent ammonium concentrations u_1 has been studied explicitly through the diagrams presented in previous sections (Figs. 2, 4, 5, and 7) and does not require further discussion here. On the other hand, the influent biomass concentration has been tacitly assumed to be zero in Equation (1), while in practice there will always be some ammonium oxidizers and nitrite oxidizers (“at least one”) present in the influent, of which the concentrations constitute additional model input variables. Biomass presence in the influent will particularly affect the occurrence of steady states that are located on the boundary of the system’s state space. It has been shown for model I and II (Volcke, 2006; Volcke et al., 2006) as well as for model IV (Sbarciog et al., 2006) that, in case ammonium oxidizers are present in the influent, the wash-out steady state \mathbf{x}_{ss}^A is only a physical steady state in case it is the *only* steady state, that is, in zone A. If nitrite oxidizers are present in the influent, the steady state \mathbf{x}_{ss}^B , corresponding with only nitrite formation, is only a physical steady state for model I and II in operating zone AB, that is, in case the steady state \mathbf{x}_{ss}^C , corresponding with nitrate formation, does not occur (Volcke, 2006), or in operating zone AB or ABCD for model IV (Sbarciog et al., 2006). Nevertheless, these effects are not very drastic, as the steady states involved are not asymptotically stable in the concerned input regions, which means they are usually not reached anyway for the corresponding combinations of influent ammonium concentrations and dilution rates.

Conclusions

In this paper, the influence of microbial growth kinetics on steady state multiplicity and stability of a nitrogen removal process has been addressed. The model under study is a two-step nitrification model, in which the maximum growth rate of ammonium oxidizers is larger than one of nitrite oxidizers, which describes the behavior of a SHARON reactor. The results agree with well-known operating rules: in order to realize only nitrite formation, the applied dilution rate should not be too high to prevent wash-out of ammonium oxidizers, but not too low to keep out nitrite oxidizers. In addition, the obtained results clearly show that the given influent ammonium concentration also plays a role.

Inhibition of ammonium oxidation by its product nitrite does not affect the number of steady states of the reactor model, neither their stability, although the position of the steady states corresponding with biomass growth changes. In contrast to product inhibition, substrate inhibition (combined with substrate limitation, resulting in Haldane kinetics) clearly is a source of additional steady states: ammonium inhibition of ammonium oxidation results in the occurrence of up to five steady states, while nitrite inhibition of nitrite oxidation gives rise to up to four steady states.

The region in the input space for which only nitrite is formed, increases in case ammonium oxidation is inhibited by nitrite; it becomes smaller in case this reaction is inhibited by ammonium. Inhibition of nitrite oxidation by nitrite overall results in a larger operating region leading to only nitrite formation.

The results in this contribution clearly demonstrate how the microbial (inhibition) kinetics affect the number and the stability of steady states of a bioreactor model. The description of microbial kinetics with respect to inhibition appears a crucial step in modeling biological processes as it may lead to very different steady state behaviors of the resulting model. Nevertheless, smooth transitions occur between different model structures. In the same sense, slightly changing parameter values only will have small effects. If a priori knowledge on microbial kinetics is available—even within a certain range of uncertainty for the parameter values—this insight can be used to predict the steady states that can be reached for given input values, dependent on the initial conditions. Vice versa, it also allows elucidating the type of microbial kinetics from experimental observations.

References

- Agrawal P, Lee C, Lim HC, Ramkrishna D. 1982. Theoretical investigations of dynamic behavior of isothermal continuous stirred tank biological reactors. *Chem Eng Sci* 37(3):453–462.
- Anthonisen AC, Loehr RC, Prakasam TBS, Srinath EG. 1976. Inhibition of nitrification by ammonia and nitrous acid. *J WPCF* 48:835–852.
- Bastin G, Dochain D. 1990. On-line estimation and adaptive control of bioreactors. Amsterdam: Elsevier. 379p.
- Bastin G, Van Impe JF. 1995. Nonlinear and adaptive control in biotechnology: A tutorial. *Eur J Control* 1:37–53.
- Carrera J, Jubany I, Carvallo L, Chamy R, Lafuente J. 2004. Kinetic models for nitrification inhibition by ammonium and nitrite in a suspended and an immobilised biomass systems. *Process Biochem* 39:1159–1165.
- Genesio R, Tartaglia M, Vincino A. 1985. On the estimation of asymptotic stability regions: State of the art and new proposals. *IEEE T Automat Control* 30:747–755.
- Hellinga C, Schellen AAJC, Mulder JW, van Loosdrecht MCM, Heijnen JJ. 1998. The SHARON process: An innovative method for nitrogen removal from ammonium-rich wastewater. *Water Sci Tech* 37(9):135–142.
- Hellinga C, van Loosdrecht MCM, Heijnen JJ. 1999. Model based design of a novel process for nitrogen removal from concentrated flows. *Math Comp Model Dyn Syst* 5(4):351–371.
- Lei F, Olsson L, Jorgensen SB. 2003. Experimental investigations of multiple steady states in aerobic continuous cultivations of *Saccharomyces cerevisiae*. *Biotechnol Bioeng* 82(7):766–777.
- Loccufier M, Noldus EN. 2000. A new trajectory reversing method for estimating stability regions of autonomous nonlinear systems. *Nonlinear Dyn* 21:265–288.
- Namjoshi AA, Ramkrishna D. 2001. Multiplicity and stability of steady states in continuous bioreactors: Dissection of cybernetic models. *Chem Eng Sci* 56:5593–5607.
- Sbarciog M, Volcke EIP, Loccufier M, Noldus M. 2006. Stability boundaries of a SHARON bioreactor model with multiple equilibrium points. *Nonlinear Dyn Syst Theory* 6(2):191–203.
- Tong CC, Fan L-S. 1988. Concentration multiplicity in a draft tube fluidized-bed bioreactor involving two limiting substrates. *Biotechnol Bioeng* 31:24–34.
- Van Hulle SWH, Volcke EIP, López Teruel J, Donkels B, van Loosdrecht MCM, Vanrolleghem PA. 2007. Influence of temperature and pH on the kinetics of the SHARON nitrification process. *J Chem Technol Biot* 82(5):471–480.
- Volcke EIP. 2006. Modeling, analysis and control of partial nitritation in a SHARON reactor. PhD thesis, Ghent University, Belgium. 300 p. Available on http://biomath.ugent.be/publications/download/VolckeEveline_PhD.pdf
- Volcke EIP, Loccufier M, Vanrolleghem PA, Noldus EIJL. 2006. Existence, uniqueness and stability of the equilibrium points of a SHARON bioreactor model. *J Process Control* 16:1003–1012.
- Wiesmann U. 1994. Biological nitrogen removal from wastewater. In: Fiechter A, editor. *Advances in Biochem Eng/Biotech*, vol 51. Berlin: Springer-Verlag. pp 113–154.